FRACTURE LENGTH SCALES IN DELAMINATION OF COMPOSITE MATERIALS

R. B. Sills[*] and M. D. Thouless[**, ***]

[*] Gas Transfer Systems, Sandia National Laboratories, Livermore, CA 94550 USA
[**] Department of Mechanical Engineering, University of Michigan, Ann Arbor, MI 48109 USA
[***] Department of Materials Science & Engineering, University of Michigan, Ann Arbor, MI 48109 USA

ABSTRACT

Cohesive zone models of fracture have seen great success in modeling delamination and debonding of composite materials (Aymerich *et al.* 2009; Li *et al.* 2005b; Yang & Cox 2005). By embedding cohesive zone elements along potential crack planes, arbitrary delamination configurations can be represented without the need for a priori knowledge of crack locations or pre-existing cracks. The stress-displacement behavior of elements in cohesive zone modeling is governed by cohesive or traction-separation laws, which dictate the tractions across the interface as a function of the crack plane separations. For mixed-mode problems, orthogonal sets of cohesive laws can define these relationships for each mode. In fibrous composites, various toughening mechanisms such as matrix cracking and fiber bridging operate at different strengths and length scales forming a complicated amalgamation of processes that are difficult to model directly. With cohesive zone modeling, these processes can be accounted for in the cohesive law via the fracture length scale. Many authors have pointed out that the shape of the traction-separation law and its associated fracture length scales is dictated by the cohesive mechanisms at work (Dávila *et al.* 2009; Li *et al.* 2005a; Yang & Cox 2005) but a general framework for understanding how the evolution of these mechanisms with loading manifest themselves within the cohesive zone structure has not been presented. In this work, such a framework will be developed by defining an average fracture length scale that is a property of the load state along the crack plane. With this new length scale, the effects of cohesive law shape can be understood – allowing a direct connection between law shape and physical process.

1. INTRODUCTION

Cohesive zone models of fracture provide a broad framework for representing material behavior during fracture or delamination. By defining the normal and shear tractions across potential fracture planes, arbitrary crack configurations can be modeled without the need for a priori

knowledge of crack locations. The relationships defining these tractions are known as cohesive or traction-separation laws and they relate the tractions to the opening displacements between the planes. An example of a traction-separation law is given in Fig. 1. The area swept out under-the-curve at any increment of load is the strain energy release rate, $\mathcal{G}$, and the net area under-the-curve is the toughness of the interface, Γ. By introducing finite stresses at the crack tip, cohesive zone models of fracture provide a means for understanding the effects of cohesive strengths on fracture (Tvergaard and Hutchinson 1992; Parmigiani and Thouless 2007). Furthermore, these finite stresses introduce a length scale absent in linear-elastic fracture mechanics (LEFM) known as the fracture length scale. This length scale is generally defined as (Hillerborg *et al.* 1976; Bao and Suo 1992)

$$\zeta_{nominal} = \frac{\Gamma E}{\hat{\sigma}^2} \tag{1}$$

where Γ is the toughness, E is the modulus of elasticity, and $\hat{\sigma}$ is the peak stress of the traction-separation law (see Fig. 1). It has been demonstrated by numerous authors that this length scale is instructive in predicting whether the Inglis (1913) strength approach to fracture or the Griffith (1920) energy approach will predict the crack behavior (Bao and Suo 1992; Parmigiani and Thouless 2007). When the fracture length scale is small compared to all physical dimensions, energy dominates the fracture process, the assumptions necessary for LEFM are valid, and the material and geometry is said to be flaw intolerant (notch sensitive). When the length scale is large, strength is the dominating property causing net-ligament failure and flaw insensitivity. If the length scale exists between these extremes, both strength and energy will play a role.

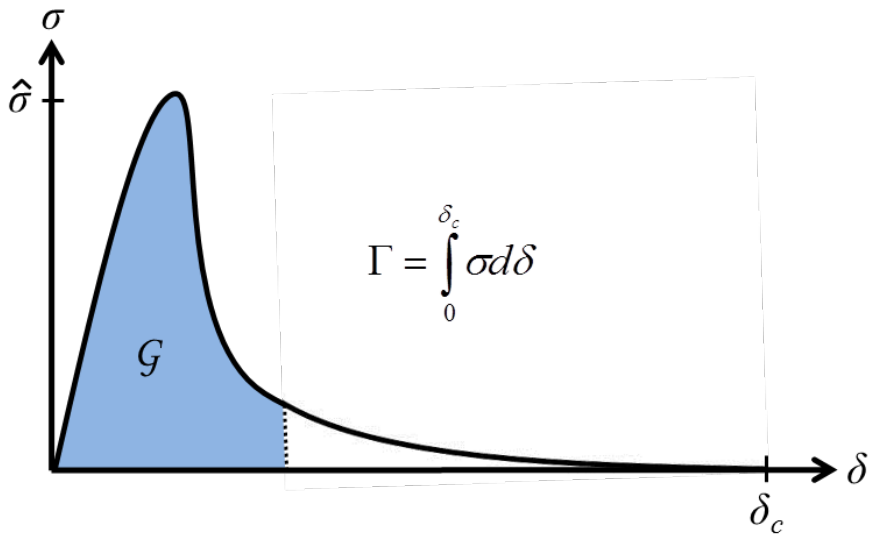

Fig. 1. A basic traction-separation or cohesive law.

Traction-separation laws can take any shape depending on the toughening and deformation processes present. Such generality allows for the accurate depiction of a broad range of materials. In the case of fibrous composite materials numerous processes contribute to the cohesive tractions including matrix cracking, fiber breakage, delamination, and pullout, and frictional sliding. The law shape can be derived by direct measurement of tractions and displacements (Sørensen and Jacobsen 1998), performing strength and toughness characterizing mechanical tests (Li *et al.* 2005b), or with micromechanical modeling (Sørensen *et al.* 2008).

Many authors have found that in modeling material systems, details regarding the shape of the traction-separation law are of secondary importance as long as the toughness and cohesive strength (peak stress) are correct - it is upon this assumption that Eqn. 1 was derived. Sills and Thouless (2011a,b) however, demonstrated that the law shape and fracture length scale are intrinsically linked. Extending the fracture length scale concept to any increment of load, they defined an instantaneous fracture length scale as

$$\zeta_{inst.} = \frac{\Gamma E}{\sigma_{ave}^2} \tag{2}$$

where σ_{ave} is the average stress of the cohesive law at the current load increment and displacement, δ, given by

$$\sigma_{ave} = \frac{1}{\delta}\int_0^{\delta} \sigma d\delta = \mathcal{G}(\delta)/\delta \tag{3}$$

With Eqn. 2, a linear traction-separation law will have an instantaneous fracture length scale that is independent of the load increment and inversely proportional to the slope. Any nonlinear cohesive law will have a changing fracture length scale as the system is loaded. In mixed-mode problems, each mode has its own fracture length scale given by the relevant displacement (normal, in-plane tangential, or out-of-plane tangential) and strain energy release rate component. How these fracture length scales combine and form an overall fracture length scale is not clear (Sills and Thouless 2011b), however it is clear that law shape must be accounted for in calculating the fracture length scale.

It should be noted that in the case of large scale bridging (when the length of the bridging zone becomes comparable to a characteristic physical dimension), the physical manifestation of the fracture length scale becomes dependent on a characteristic physical dimension (Bao and Suo 1992; Yang and Cox 2005). This is due to the fact that the compliance of the system limits the development of the process zone. In this work, the fracture length scale will be examined independent of specimen size and geometry.

A large effort has been put forth to understand the fracture length scale in the context of delamination in composite materials. Most of the relationships given in the literature are derived upon the assumption that law shape is of secondary importance and no work to date, to the authors' knowledge, takes into account the evolution of the fracture length scale with loading. The impetus for this work is then to understand the behavior of the fracture length scale during delamination in composites.

2. DESCRIPTION OF THE DELAMINATION PROCESS

The delamination behavior of composites can vary greatly as a function of the fiber and matrix materials, fiber volume fraction, ply composition and orientation, and the specimen geometry. In general, however, the process can be decomposed into two stages: matrix cracking and fiber bridging. Matrix cracking initiates the delamination process and is generally considered to occur in a manner consistent with linear-elastic fracture mechanics – the toughness of the fiber-reinforced matrix dominates crack growth. Following the matrix crack, fibers can bridge the crack opening for a significant amount of growth as they undergo debonding, pull-out, and

frictional sliding. The bridging portion of the crack growth process is often considered within the context of a bridging law, which dictates the tractions applied by the bridging fibers as a function of the crack face displacements in the same way a cohesive law does. Cohesive and bridging laws differ only in how their abscissa is defined – cohesive laws describe the entire delamination process while bridging laws only focus on crack growth after the matrix crack has formed; this work focuses on the former. From a computational point of view cohesive laws are more useful because they allow cracks to be modeled easily from an equilibrium (unloaded) state.

Many authors have noted that the various portions (displacement regimes) of traction-separation laws for composite materials can be thought of as representing different toughening and deformation mechanisms (Dávila *et al.* 2009; Gutkin *et al.* 2011; Li *et al.* 2005b; Yang and Cox 2005) – this work will make use of this observation as follows. Before matrix cracks develop or grow, the system behaves in a linearly elastic manner with the opening behavior being dictated primarily by the matrix and fiber moduli and the fiber volume fraction. Matrix cracks then form, either on their own or due to fiber debonds, and grow up to when the matrix strength, $\hat{\sigma}_m$, and toughness, Γ_m, are reached. The crack faces are then primarily supported by fiber ligaments that bridge between them, providing tractions that start at some peak bridging value, $\hat{\sigma}_b$, and decay to zero as the strain energy release rate approaches the sum of the matrix and bridging toughness, Γ_b. This simple description of the delamination process can be represented by the tri-linear cohesive law in Fig. 2. With this model, matrix cracking dominates the stress-displacement behavior when the opening displacement, δ, is less than δ_m. Beyond this value, fiber bridging governs the response until all of the fibers fully pull-out or break at the critical displacement, δ_c.

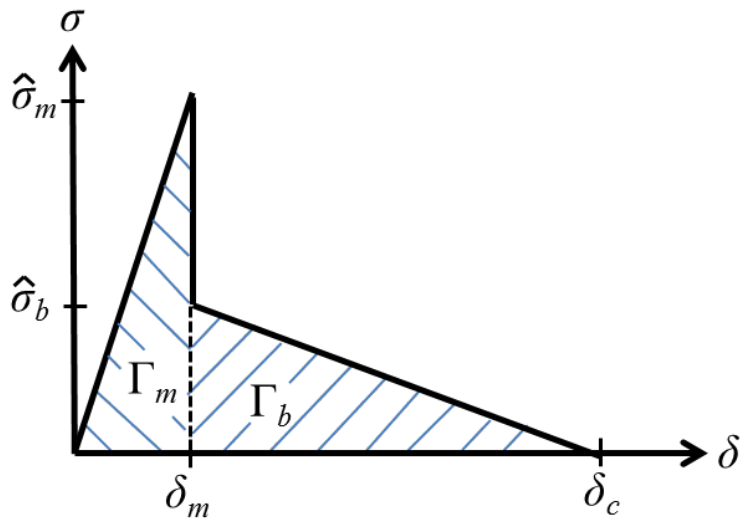

Fig. 2. The traction-separation law used to model composite delamination in this work. Subscripts *m* and *b* represent matrix cracking and fiber bridging, respectively.

3. COHESIVE LAW FORMULATION

For a general tri-linear cohesive law, the traction-separation law has the piecewise form (Gutkin et al. 2011):

$$\sigma(\delta)=\begin{cases}\dfrac{\hat{\sigma}_1}{\delta_1}\delta^2 & 0\le\delta\le\delta_1\\ \dfrac{\hat{\sigma}_1}{\delta_2-\delta_1}\left[\left(\dfrac{1}{R}-1\right)\delta+\left(\delta_2-\dfrac{\delta_1}{R}\right)\right] & \delta_1<\delta\le\delta_2\\ \dfrac{\hat{\sigma}_1}{R(\delta_c-\delta_2)}(\delta_c-\delta) & \delta_2<\delta\le\delta_c\end{cases} \tag{4}$$

where the subscripts 1 and 2 denote the ends of the first and second linear segments and R is the strength ratio, $\hat{\sigma}_1/\hat{\sigma}_2$. For this work, the differentiation between the displacements δ_1 and δ_2 is unnecessary and so to reduce the number of parameters all results will be derived with $\delta_1=\delta_2$.

As discussed above, the cohesive law used in this work will represent matrix cracking followed by fiber bridging. This formulation is convenient because it is a direct analog to much of the fiber bridging literature, which considers a toughness at the crack tip (matrix cracking) and a toughness and strength in the bridging zone. In order to fully define the law shape, four of the following six parameters must be specified:

$$\hat{\sigma}_m \qquad \hat{\sigma}_b \qquad \Gamma_m \qquad \Gamma_b \qquad \delta_m \qquad \delta_c$$

where the first four retain the definition used above, δ_m is the displacement after full matrix crack-dominated growth, and δ_c is the critical displacement upon complete fiber-ligament failure. These variables are depicted in Fig. 2.

4. FRACTURE LENGTH SCALES

By using Eqn. (4) in Eqn. (3) and applying the result to Eqn. (2), the instantaneous fracture length scale for our model traction-separation law as a function of the opening displacement is given by

$$\zeta/\delta_c=\begin{cases}2\left(\dfrac{E^*}{\hat{\sigma}_m}\right)\left(\dfrac{G}{R+G}\right) & 0\le\delta\le\delta_m\\ \left(\dfrac{E^*}{\hat{\sigma}_m}\right)\left(\dfrac{\delta}{\delta_c}\right)^2\left(\dfrac{G}{R+G}\left(\dfrac{1}{2}-\dfrac{1}{R}-\dfrac{G}{2R^2}\right)+\dfrac{\delta}{\delta_c}\left(\dfrac{1}{R}+\dfrac{G}{R^2}\right)-\dfrac{1}{2}\left(\dfrac{\delta}{\delta_c}\right)^2\dfrac{R+G}{R^2}\right)^{-1} & \delta_m<\delta\le\delta_c\end{cases} \tag{5}$$

where $G=\Gamma_m/\Gamma_b$, the toughness ratio, $R=\hat{\sigma}_m/\hat{\sigma}_b$, the strength ratio, and E^* is the effective modulus. Note that the two key displacements are related by $\delta_m/\delta_c=G/(R+G)$. For a bimaterial interface crack, the effective modulus is $2\overline{E}_1\overline{E}_2/(\overline{E}_1+\overline{E}_2)$, where the subscripts 1 and 2 denote the two materials (Sills and Thouless 2011b). Eqn. (5) provides a simple formulation for understanding the effects of relative changes in toughness and strength on the fracture length scale.

Fracture length scales have been calculated using Eqn. (5) for a variety of toughness and strength ratios – changing these parameters can be thought of as modifying the matrix or fiber material, or the interface between the two. Fig. 4 presents how the fracture length scale evolves with loading (displacement) for toughness ratios of G=1, 10, 100, strength ratios of R=1, 10, 25,

50, 100 and with $E^*/\hat{\sigma}_m = 1$. In all cases, the length scale starts small during the matrix cracking phase and grows with loading as fiber bridging takes over up to a peak value at fracture ($\delta=\delta_c$). For values of R less than 1, the length scale will actually shrink for some portion of loading but the overall behavior is not appreciably different. All cases begin with the length scale assuming a constant value due to the initial linear portion of the traction-separation law, as discussed above. When the matrix toughness is small relative to the fiber bridging toughness (small G), the fracture length scale at fracture is highly sensitive to the strength ratio, taking larger values as the matrix becomes significantly stronger than the bridging fibers. As the toughness ratio grows, the length scale growth becomes less pronounced and less sensitive to R eventually becoming independent of it – in the limiting case, the cohesive law has a pure linear hardening shape and the fracture-length scale is completely independent of load.

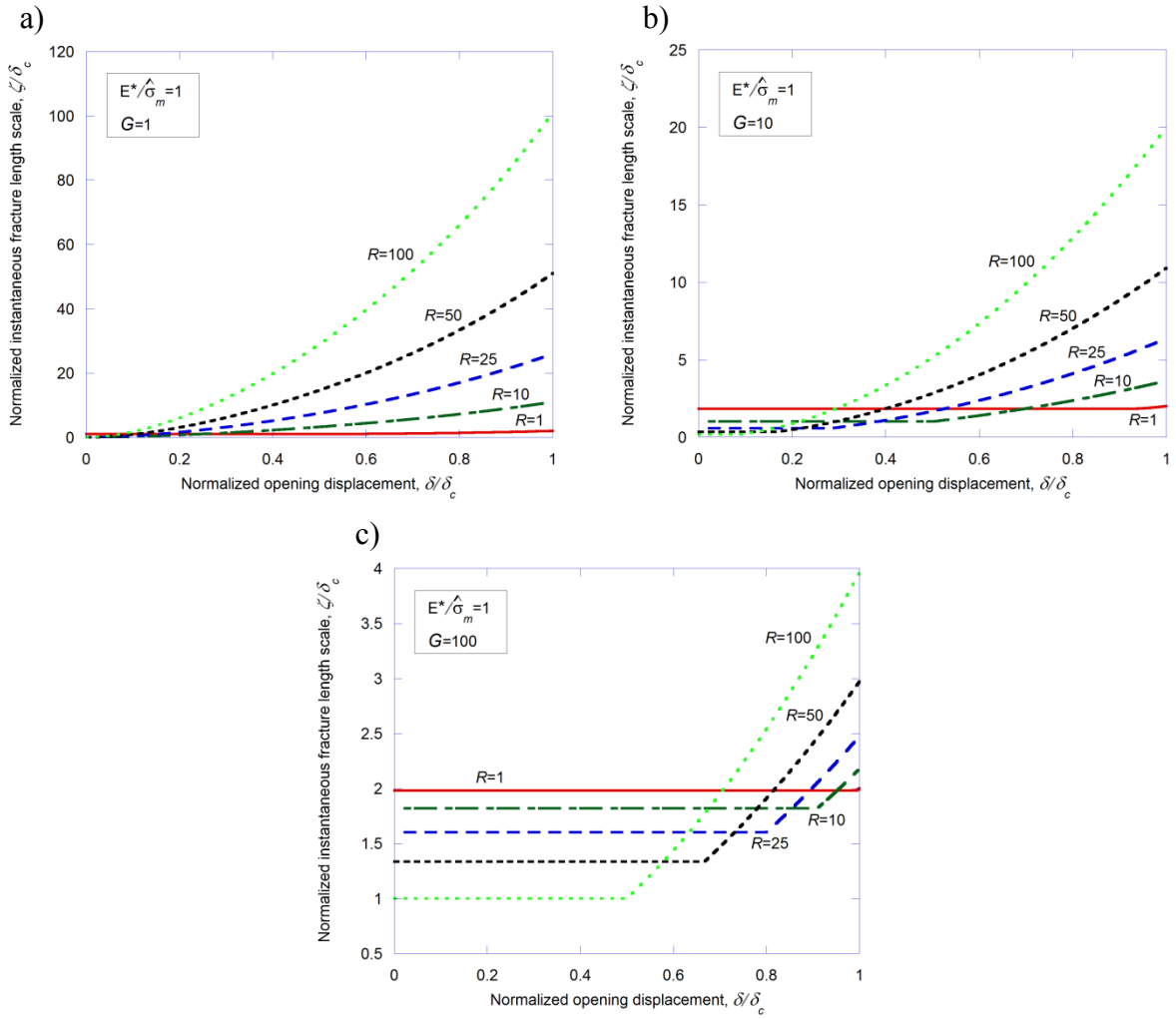

Fig. 3. The fracture length scale of the model traction-separation law depicted in Fig. 2 when $E^*/\hat{\sigma}_m = 1$, R=1, 10, 25, 50, and 100 and G=1(a), 10(b), and 100(b).

To further understand how the fracture-length scale behaves, values at fracture have been calculated and plotted in Fig. 4. In this plot, it can clearly be seen that the length scale shrinks rapidly as matrix cracking toughens relative to fiber bridging. A similar trend has been elucidated by Cox and Marshall (1994) in considering the ratio of the toughness at the crack tip to the bridging zone – their length scale assumes a bridging law with a constant bridging stress and in the notation of this work can be expressed as

$$\zeta(\delta_c)/\delta_c = \frac{\pi}{4}\left(\frac{E^*}{\hat{\sigma}_m}\right)R\left[\sqrt{1+G}-\sqrt{G}\right]^2 \tag{6}$$

This expression applies to small-scale bridging where the fracture process is fully characterized by energy considerations – the stresses at the crack tip are singular and when G is of order unity. Eqn. (6) has also been plotted in Fig. 4 with R=1000 – the curve approximately matches the results from this work around $G\approx1$, as expected.

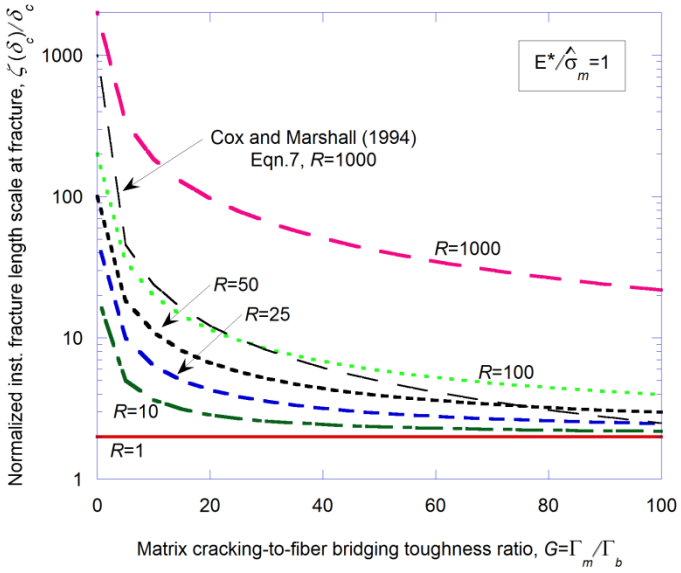

Fig. 4. The fracture length scale at fracture of the model traction-separation law depicted in Fig. 2 as a function of the toughness ratio, $G=\Gamma_m/\Gamma_b$, when $E^*/\hat{\sigma}_m = 1$ and R=1, 10, 25, 50, 100, and 1000.

It can also be seen that the strength ratio strongly affects the length scale at fracture when the toughness ratio is small – increasing the strength ratio by an order of magnitude results in a corresponding increase in the fracture length scale. This is due to the fact that when the matrix cracking strength is significantly higher than the fiber bridging strength, the interface softens significantly in transitioning between the mechanisms, and in general softening grows the fracture length scale. At large toughness ratios, the strength ratio becomes less important and in the limiting case doesn't matter all as discussed above. It is important to keep in mind that for all of these results, the effective modulus has been held constant relative to the matrix strength.

In delamination models that use bridging laws, fracture length scales are generally only considered with respect to the bridging phenomenon. Indeed, the entire benefit in using bridging models stems from the distillation of processes at the crack tip down to a strain-energy release rate and corresponding toughness, bypassing direct modeling of the large stress gradients therein (Cox and Marshall 1994). Calculating length scales in this way, however, ignores the contribution of the finite crack tip strength. Eqn. (2) dictates that the fracture length scale is a function of the entire loading history of the system, so neglecting the crack tip can result in incorrect length scales.

Cohesive laws of the form in Fig. 2 have been derived and used by numerous authors in order to represent mode I delamination and the R-curve behavior of composites. While some authors have noted that such laws work because they accurately capture the fracture mechanisms, how these mechanisms manifest themselves in the models has not been thoroughly explained. Fig. 3

presents evidence that these mechanisms affect the simulation by changing the fracture length scale, indicating that the length scale is a dynamic variable of the model. Therefore, the instantaneous fracture length scale provides an explanation for how cohesive zone modeling accurately captures the delamination process – the dynamics of strengthening and toughening are represented by changes in the fracture length scale.

REFERENCES

Aymerich, F., Dore, F., and Priolo, P. (2009). Simulation of multiple delamination in impacted cross-ply laminates using a finite element model based on cohesive interface elements. Comp. Sci. Tech. 69, 1699-1709.

Bao, G. and Suo, Z. (1992). Remarks on crack-bridging concepts. App. Mech. Rev. 45, 355-366.

Cox, B.N. and Marshall, D.B. (1994). Concepts for bridged cracks in fracture and fatigue. Acta metall. mater. 42, 341-363.

Dávila, C.G., Rose, C.A., and Camanho, P.P. (2009). A procedure for superposing linear cohesive laws to represent multiple damage mechanisms in the fracture of composites. Int. J. Fract. 158, 211-223.

Griffith, A.A. (1920). The phenomenon of rupture and flow in solids. Phil. Trans. Roy. Soc. A221, 163-198.

Gutkin, R., Laffan, M.L. Pinho, S.T., Robinson, P., and Curtis. P.T. (2011). Modelling the R-curve effect and its specimen-dependence. Int. J. Sol. Struct. Doi: 10.1016/j.ijsolstr.2011.02.025.

Hillerborg, A., Modéer, M., and Petersson, P.E. (1976). Analysis of crack formation and crack growth in concrete by means of fracture mechanics and finite elements. Cem. Con. Res. 6, 773-782.

Inglis, C.E. (1913). Stresses in a plate due to the presence of cracks and sharp corners. Proc. Inst. Nav. Arch. 55, 219-230.

Li, S., Thouless, M.D., Waas, A.M., Schroeder, J.A., and Zavattieri, P.D. (2005a). Use of mode-I cohesive-zone models to describe the fracture of an adhesively-bonded polymer-matrix composite. Comp. Sci. Tech. 65, 281-293.

Li, S., Thouless, M.D., Waas, A.M., Schroeder, J.A., and Zavattieri, P.D. (2005b). Use of cohesive-zone model to analyze the fracture of a fiber-reinforced polymer-matrix composite. Comp. Sci. Tech. 65, 537-549.

Parmigiani, J.P. and Thouless, M.D. (2007). The effects of cohesive strength and toughness on mixed-mode delamination of beam-like geometries. Eng. Fract. Mech. 74, 2675-2699.

Sills, R.B. and Thouless, M.D. (2011a). The effect of cohesive law shape on the strength of interfaces. (to be submitted).

Sills, R.B. and Thouless, M.D. (2011b). The effects of cohesive-law parameters on mixed-mode fracture. (to be submitted).

Sørensen, B.F., and Jacobsen, T.K. (1998). Large-scale bridging in composites: R-curves and bridging laws. Comp. Part A 29A, 1443-1451.

Sørensen, B.F., Gamstedt, E.K., Østergaard, R.C., and Goutianos, S. (2008). Micromechanical model of cross-over bridging – Prediction of mixed mode bridging laws. Mech. of Mat. 40, 220-234.

Tvergaard, V. and Hutchinson, J.W. (1992). The relation between crack growth resistance and fracture process parameters in elastic-plastic solids. J. Mech. Phys. Sol. 40, 1377-1397.

Yang, Q. and Cox, B. (2005). Cohesive models for damage evolution in laminated composites. Int. J. Fract. 133, 107-137.